ARTICLE NO. 79-0394R

# CCD Star Sensor for Fine Pointing Control of Spaceborne Telescopes

R.H. Stanton* and R.E. Hill†
*Jet Propulsion Laboratory, Pasadena, Calif.*

**A star sensor for measuring small pointing errors in astronomical telescopes is described. By using solid-state imaging arrays (CCD's) to track guide-star images, this design realizes a number of performance advantages relative to more conventional approaches. Specific topics include star image position measurement, CCD sensitivity including color effects, and performance simulation results. Experimental results for CCD's operating at temperatures below 100 K are also summarized. Two telescope configurations are considered to illustrate the range of possible applications of this technology: 1) a large orbiting telescope for general astronomy requiring a multi-CCD sensor, and 2) a Space Shuttle-based infrared observatory operating at 20 K. Although the requirements and configurations of these applications are widely different, the CCD approach offers substantial advantages to both systems.**

## Introduction

FINE pointing control of large astronomical telescopes in space requires star trackers of extreme accuracy and stability. Pointing errors as small as a few percent of a star image diameter must be measured and corrected to prevent the resulting image motion from significantly degrading image quality. In this paper, we describe a general fine pointing sensor (FPS) design approach which uses charge coupled device (CCD) imaging arrays to track focal plane star images. Since CCD's provide accurate positional information regardless of where the image falls within the field-of-view, the proposed sensor design can accommodate wide variations in guide-star geometry without moving parts. This advantage, coupled with the fact that several stars can be tracked simultaneously (using one or several CCD's), makes the CCD approach a strong candidate for application to a variety of future space-based astronomical telescopes now being planned by NASA.

CCD imaging arrays have several qualities which make them attractive for star tracking. A natural coordinate system is defined by the array of photosensitive elements which are not dependent on electromagnetic deflection fields (as in the case for vidicons and image dissectors). Other advantages include high sensitivity, low operating voltage and the ability to survive exposure to strong light. The quantum efficiency of these detectors, combined with their efficient use of signal integration time (all elements integrate simultaneously), makes the noise performance of CCD trackers generally competitive with other approaches limited only by quantum noise (photon counting). In many cases, further noise reductions may be achieved by tracking several stars, simultaneously, on a single CCD.[1]

One potential limitation of using CCD's for star tracking is the limited number of sensing elements (pixels) available with present arrays. Currently, the maximum array size is in the range of 500 to 800 elements on a side. These arrays will fall far short of the resolution needed for FPS applications (10,000 or more on a side). However, it is possible to achieve a substantial gain in effective resolution using interpolation. This technique has been demonstrated in CCD-based instruments developed at the Jet Propulsion Laboratory.[2,3] If a light from a star is spread over a number of adjacent CCD pixels, the relative optical intensity in these elements gives a powerful measurement of where the optical centroid lies within a particular element. This interpolation (or center finding) technique is capable of extending the effective sensor resolution between one and two orders of magnitude beyond that defined by the CCD pixel dimensions.

In addition to the requirement for sub-pixel interpolation, the fine pointing sensor provides many other design challenges. Several CCD's must be operating simultaneously in the focal plane in order to achieve adequate tracking field coverage. The capability for tracking moving targets, and even star images which have been intentionally smeared, must be provided. In some cases the bandwidth requirement for the FPS application requires integration periods of less than 25 ms. This necessitates a number of time-saving measures, such as the selective readout of only those CCD regions containing guide-star images. High-speed operation, combined with the complexities of multi-CCD coordination, has greatly increased sensor control and processing requirements beyond first generation CCD trackers. As a result, it has been necessary to replace the 8-bit microprocessors used on early designs[3] with a high-speed, 16-bit bipolar processor.

All of these improvements have been embodied in the CCD FPS design described here. Before examining specific applications of this technology, we briefly discuss the overall approach, sub-pixel interpolation and results of star detection analyses. These results serve as a basis for a discussion of two important telescope applications: 1) a large free-orbiting telescope for general astronomy, and 2) a Shuttle-based infrared observatory.

## Sensor Description

### Configuration

The FPS employs one or more CCD detectors operating under processor control to provide error signals to the pointing control system. Figure 1 illustrates this overall structure. Processor functions include the following elements:

*CCD readout control:* Commands issued to a hard-wired scan controller determined which CCD's are read out and where each star is expected in CCD coordinates. The scan

Presented as Paper 79-0394 at the 17th Aerospace Sciences Meeting, New Orleans, La., Jan. 15-17, 1979; submitted Feb. 20, 1979; revision received July 30, 1979. 

Index categories: Sensor Systems; Guidance and Control.

*Supervisor, Celestial Sensors Group, Guidance and Control Section.

†Contract Engineer.

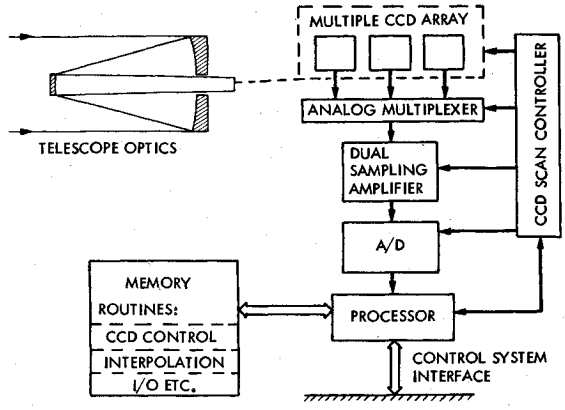


**Fig. 1 FPS block diagram.**

controller then provides the necessary timing pulses to assure that the selected CCD elements are sampled, encoded and sent to the processor.

*Data gathering:* Digital intensity data (12 to 16 bits/pixel) from the CCD is stored until all guide-stars have been sampled.

*Image interpolation:* Once all star data are read, the processor calculates the centroid of each image, applies corrections for distortions in the optics or interpolator nonlinearities, etc., and outputs the measured offset $(\Delta X, \Delta Y)$ between the observed and desired star coordinates. If desired, pitch-yaw-roll errors can also be calculated based on simultaneous tracking of two or more star images.[4]

*Mode selection:* The processor determines whether the sensor is looking for stars (acquisition) or tracking images already known to be at specific locations in CCD coordinates (track).

*Input/output:* All data interfaces with the rest of the spacecraft are under processor control. This includes error signal output, parameter and mode selection input, and software uploading.

### Operating Modes

*Acquisition*

Each CCD array expected to contain guide-star images is scanned during the acquisition mode to locate the stars to be tracked. Stars are initially selected on the basis of intensity, with final identification based on star-pair separation. Once stars are acquired and identified, error signals, based on the difference between the desired and observed guide-star coordinates, are sent to the telescope control system to permit telescope repointing. Track-mode is entered only after repointing has brought guide-stars to within approximately one CCD pixel of their desired locations.

*Track*

The tracking of stars acquired during the acqusition mode provides data for calculation of pointing error signals. Since star image pixel coordinates are known, only those regions of the CCD containing guide-star images need to be read out and encoded. This enables high-speed operation (up to 40 cycles/second) while still maintaining relatively long sampling times ($>10\ \mu s$/pixel) for readout of those CCD cells actually containing a star image. Note that the tracking of moving targets (i.e., solar system bodies that move with respect to the guide-stars) can be easily accomplished in the track mode by appropriate adjustments of the desired guide-star coordinates.

### Image Centroid Algorithm

An interpolation algorithm is used to achieve resolution better than the detector pixel-to-pixel spacing. The algorithm must be simple so it can be executed in real-time with relatively little onboard computational capability. It must also be accurate, with minimum nonlinearity in both $X$ and $Y$ directions across a pixel, and finally, it must minimize sensitivity to noise.

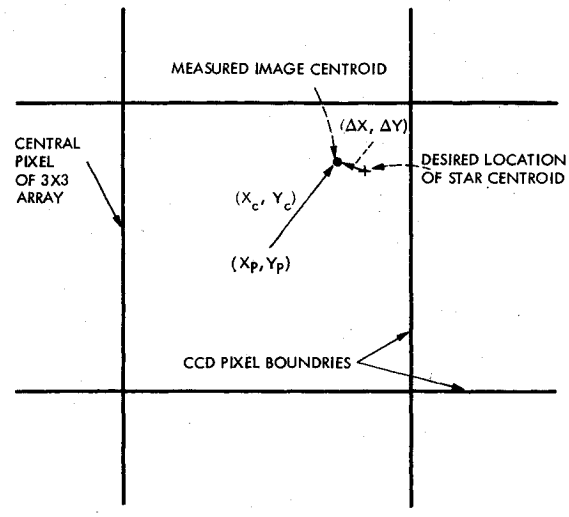


**Fig. 2 Star image centerfinding coordinate system within a single CCD pixel.**

A simple center-of-brightness algorithm has been found to meet these requirements. This is a modification of the algorithm used for the STELLAR tracker[2] using an interpolation subarray size of $3\times3$ pixels. The subarray center is the origin of the interpolation coordinate system. Thus, every star image location is specified by giving the coordinates $x_p$ and $y_p$, of the subarray center and the interpolated position $x_c$ and $y_c$, within the central pixel of the subarray (Fig. 2).

With this algorithm, the difference in measured image intensity between the first and third columns (or rows) of the subarray provides a sensitive measure of image location:

$$x_c = (A_1/S)(Sx_3 - Sx_1) \qquad y_c = (A_2/S)(Sy_3 - Sy_1) \quad (1)$$

where

$$Sx_j = \sum_i I_{ij} \qquad Sy_i = \sum_j I_{ij} \quad (2)$$

and

$$S = \sum_{ij} I_{ij} \quad (3)$$

The measured light intensity for each pixel, $I'_{ij}$, is corrected for background effects by subtraction of a small threshold $K$ prior to use in Eqs. (2) and (3)

$$I_{ij} = \begin{cases} I'_{ij} - K & \text{if } I'_{ij} > K \\ 0 & \text{otherwise} \end{cases} \quad (4)$$

This subtraction has the effect of removing any centroid bias caused by background video level, as well as removing the noise associated with pixels not contributing significantly to centroid determination.

The constants $A_1$ and $A_2$ depend on the size of the effective optical image diameter, being close to unity for an image slightly larger than one CCD element in diameter. This size represents a lower limit since a smaller image could be completely contained within one pixel, providing no information for the interpolator. On the other hand, large images have two disadvantages: 1) measurement noise (centroid jitter) varies proportionally with the optical image diameter; and 2) images larger than 2 pixels in diameter would "spill" out of the $3\times3$ submatrix for some locations.

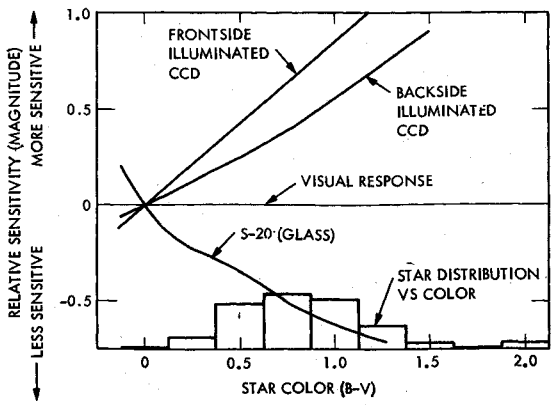


**Fig. 3 Relative response of sensors vs star color and star distribution near the galactic pole.**

The linearity of the interpolation calculation depends on the linearity of the star image edge-trace function and the modulation transfer function (MTF) of the CCD. Linearity of response is not important in some applications where only a nulling signal is required, but in others requiring an accurate proportional error signal, it is of considerable importance. In general, the central obscuration present in most reflecting telescope designs improves this characteristic. Measurements of laboratory optics and theoretical evaluation of defocused images suggest that edge-trace linearity of ±4% (between 10 and 90% points) can be readily achieved for images of the required diameter (~30 μm).

#### Star Detection

A critical factor affecting the feasibility of any FPS design is the detection of an adequate number of guide-stars. This is particularly true for the CCD-based approach since it relies on covering the guide-star field with fixed detectors rather than moving elements (mirrors, detectors, etc.) to accommodate star pattern variations. Thus, the greater the density of available stars, the smaller the area (fewer CCD's) that must be covered to achieve acceptable probability of finding adequate guide-stars.

To determine the average number of stars available for a particular sensor geometry, two related factors must be evaluated. First, the CCD response to stars must be known as a function of star spectral class (color). This permits calculation of magnitude thresholds and evaluation of color effects. Secondly, the density of background stars, taking into account variations in star color, must be calculated.

Figure 3 shows the relative response of three different sensors as a function of star color. The difference, in magnitude, $\Delta M$, is plotted against a standard color index ($B$-$V$), which increases for cooler (redder) stars. The distribution of guide-stars (vs color) is also shown. Two different CCD's are plotted to indicate the range between frontside illumination (where incoming starlight passes through the CCD polysilicon gate structure) and backside illumination (where the light impinges on pure silicon). It must be emphasized that these give *relative* response, with the difference between sensors arbitrarily set to zero at zero color (spectral class A0). A comparison between devices in terms of output signal for a fixed star magnitude input is given in Table 1.

**Table 1 Photodetector response**

| Sensor | Response[a] |
|---|---|
| S-20 photocathode | ~120 e/cm$^2$ – s |
| Frontside CCD | ~500 e/cm$^2$ – s |
| Backside CCD | ~670 e/cm$^2$ – s |

[a] Response is given in photoelectrons/cm$^2$ of optical aperture for a 9th magnitude A0 star.

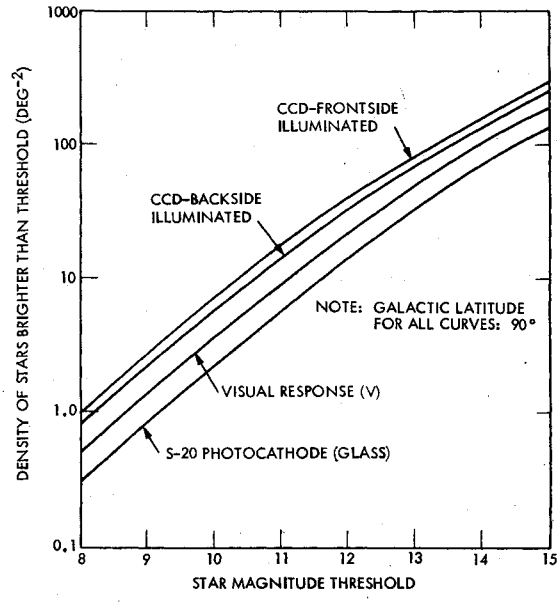


**Fig. 4 Density of available background stars for CCD and photocathode-based sensors vs detection threshold for AO stars.**

The trend of the curves shown in Fig. 3 can be readily understood. The excellent red response (out to 1.1 μm) of CCD's gives a considerable advantage for red stars (high B-V) relative to the human eye. Conversely, common photocathodes, with their strong response in the blue, become relatively less sensitive to red stars than the eye.

These factors become important when the distribution in color of potential guide-stars is taken into account. In regions of poorest star background (i.e., high galactic latitude) there is a significant predominance of red stars, as can be seen on the bar graph in Fig. 3.[5,6] This predominance, when combined with greater red response of CCD's, leads to more available stars for a given threshold magnitude using a CCD than the standard star density tables, measured with respect to the visual response function, would indicate. Again, the converse is true for an S-20 photocathode-based instrument.

These differences are summarized in Fig. 4, which presents the density of available background stars vs. threshold magnitude for the sensors described earlier. Only data for the galactic polar regions are plotted, giving a measure of worst-case guide-star availability. The factor of 2 gain in available background star density for a CCD-based instrument is significant since it may result in a substantial reduction in the focal plane area required for the FPS function.

## FPS Applications

Two applications of the CCD fine pointing sensor are considered in this section: 1) a large free-orbiting telescope for general astronomy, and 2) a Shuttle-based infrared observatory. These examples illustrate the wide range of uses for this technology without by any means exhausting the possibilities. Although the difference in focal plane geometry is substantial, in both cases a CCD-based sensor is capable of generating the required fine pointing error signals.

**Table 2 Free-orbiting telescope—FPS requirements**

| | |
|---|---|
| Telescope optics | |
| Diameter | 2.5 m |
| Focal ratio | $f/25$ |
| Available tracking field | Annulus ($R$ = 10-14 arcmin) |
| Required FPS sensitivity | Detect 14-15 magnitude stars |
| Accuracy | ±0.01 arcsec |
| Stability | 0.003 arcsec (1$\sigma$) |
| Output data rate | 40/s |
| Maximum track rate | 0.25 arcsec/s |

**Table 3 CCD/system parameters**

| | |
|---|---|
| Format | 500 × 500 elements |
| Pixel size | 24 μm square |
| Sensitivity | 50% peak quantum efficiency (frontside illumination) |
| Noise | 25 electrons/pixel |
| Saturation | 150,000 electrons/pixel |
| Output quantization (D/A conversion) | 12 bits (14 bits equivalent for $M > 11$) |
| Operating temperature | ~ −20°C (thermoelectrically cooled) |

**Free-Orbiting telescope**

In order to quantitatively evaluate the expected FPS performance for this application, a specific telescope configuration was assumed. This configuration and performance requirements identified for the FPS are summarized in Table 2. Note that it is assumed that the available tracking field is located on the periphery of the science instrument field in an annulus between 10 and 14 arcmin from the optical axis. This configuration assures a maximum utilization of the high-quality field (near the optical axis) for scientific purposes.

Table 3 summarizes the CCD characteristics used in this evaluation. Although not identical with any CCD that is currently available, the characteristics listed are typical of devices now produced or under development by a number of manufacturers.

Due to the long focal length of the telescope optics, there is a substantial mismatch between the size of the available tracking field and the physical dimensions of existing CCD's. To circumvent this problem, an optical image-scale reduction of 5× was introduced to provide a match between the radial width of the telescope tracking field and the CCD dimensions. This allows the tracking field area to be covered effectively by as many as 12 CCD's (Fig. 5). Whether this many CCD's are actually needed depends on what percentage of the time the sensor must detect adequate guide-stars under worst-case conditions (see following section).

**Performance Simulation**

A number of computer simulations were developed to predict sensor tracking performance as a function of FPS design variables. Image intensity distributions for the incident star images were calculated for a variety of reduction optics designs (Fig. 6 illustrates one approach). System parameters, including CCD sensitivity and noise, A/D quantization, and processor quantization and roundoff were accurately simulated. Simulation outputs include both systematic interpolation errors (nonlinearities) and rms noise expected as a function of input parameters.

Figure 7 illustrates the predicted interpolation output noise for a faint ($m \sim 14.2$) star image located at three different

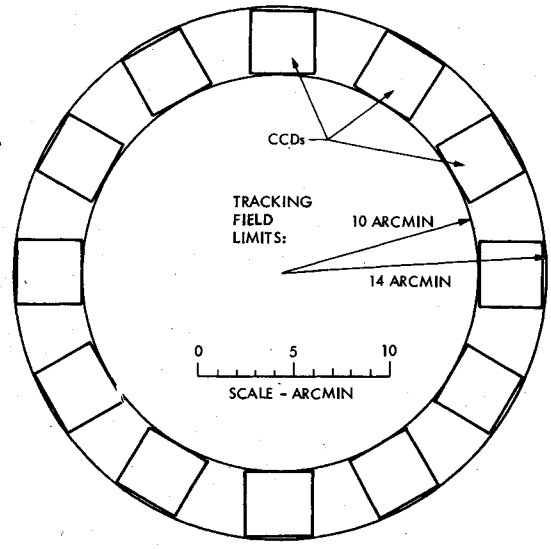


**Fig. 5 Guide field geometry in telescope image plane.**

positions within a single CCD pixel. Note that the limited resolution of the analog-to-digital conversion (14 bits) results in a quantization of interpolator output. Note also that the noise does not depend strongly on where in the pixel the star centroid is located.

Average interpolation noise is plotted in Fig. 8 as a function of star magnitude for two integration intervals (18 and 43 ms). These times correspond to update frequencies of 40 and 20 Hz, respectively, due to a fixed 7 ms required to read out the CCD data.

To interpret these results in terms of the probability of achieving a given error signal stability for an arbitrary telescope pointing direction, it is necessary to consider several additional factors: 1) the available background star density as a function of magnitude (Fig. 4), 2) the area of sky actually covered by the CCD configuration (Fig. 5), 3) the expected tracking accuracy as a function of magnitude (Fig. 8), and 4) the maximum number of stars that can be tracked at a given time.

In order to correctly weigh the contribution of stars of each magnitude, a Monte Carlo analysis was performed by randomly generating 10,000 star configurations corresponding to known mean densities. For each configuration, the error signal stability resulting from tracking the four brightest stars in the field was calculated. A ranking of the results produced the curves in Fig. 9 which show the expected error signal noise in arcsec vs the probability that adequate guide-stars are available to achieve that noise level. Three cases are plotted showing both the effect of doubling the number of CCD's

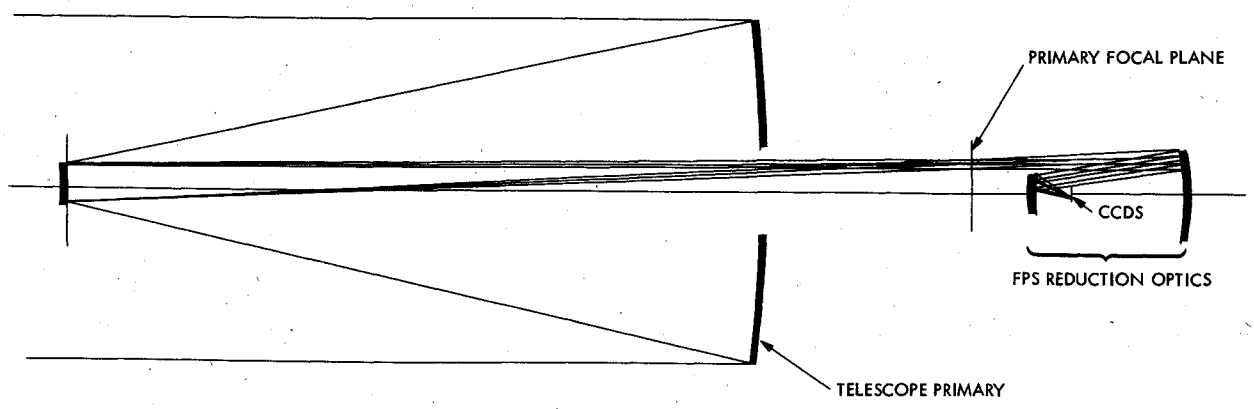


**Fig. 6 Image scale reducing optics—two mirror example.**

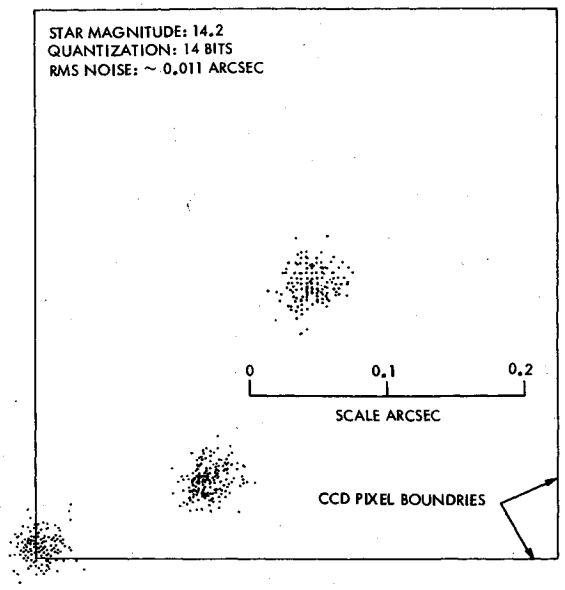


**Fig. 7 Example of simulated output noise for tracking a faint star image.**

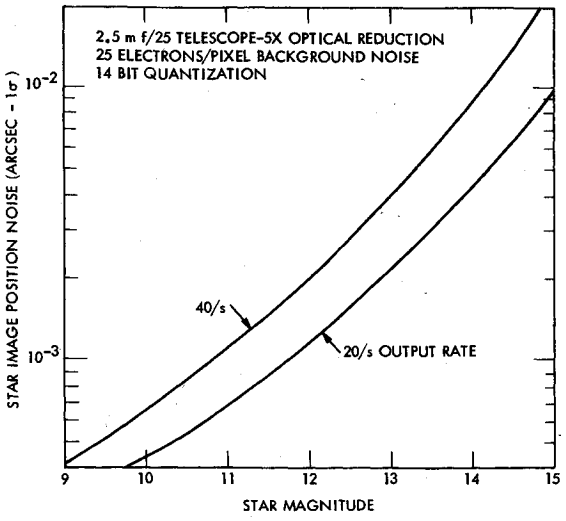


**Fig. 8 Calculated star position measurement noise.**

used and the result of halving the output data rate from 40 to 20/s.

A comparison between Fig. 9 and Table 2 shows that the required error stability is achieved for 71% of all cases at the high rate (40/s) using only 6 CCD's, and for over 90% of all pointing directions if 12 CCD's are used, or if the output data rate is halved (20/s). Note that this performance is achieved when the telescope is pointing in the direction where the star background is poorest (i.e., toward the galactic pole). Thus, a CCD-based FPS can be tailored to provide low noise performance with a high probability of success even for regions with few background stars.

### Shuttle-Based Infrared Telescope

FPS requirements for infrared telescopes are somewhat different from those for short wavelength instruments. Telescopes cooled to cryogenic temperatures for the 5-30 $\mu$ range are characterized by comparatively small aperture, short focal length, wide field and less stringent angular pointing requirements. As IR observations are concerned only with long wavelength regions, a dichroic reflector can be used to separate out the visible wavelength portions for use in guiding, while the longer wavelengths are directed to the

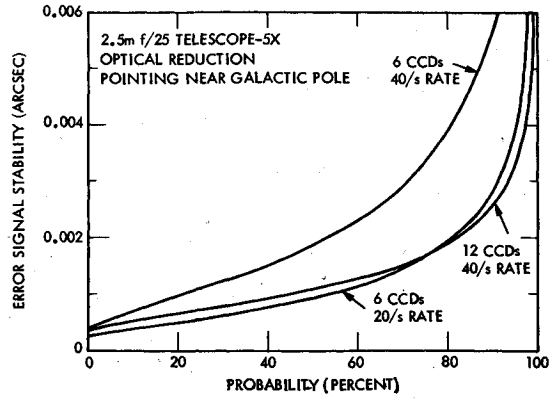


**Fig. 9 Expected error signal noise including the improvement associated with tracking several stars simultaneously.**

science instruments. This permits the FPS to share the central instrument field with the scientific instruments, giving the tracking function access to high-quality images.

Infrared telescopes also impose additional performance requirements on the fine pointing sensor. Typical requirements are summarized in Table 4. First, IR mapping of distributed sources in space necessitates a raster scan motion of the telescope relative to the guide-stars. In order to limit the streak images of the guide-stars to manageable limits, a moderately high sampling rate in the FPS is required. Secondly, it is often necessary to "chop" the incoming radiation by periodically displacing the telescope axis from the target star to a dark region in space. This chopping action also displaces the guide-star images on CCD, giving each star two images corresponding to the extremes of the chop motion. As guide-star measurements are used to control the motion of the chopping mirror, the FPS is designed to track these double images. Finally, the CCD operation must be compatible with the telescope cryogenic environment.

### Low-Temperature CCD Operation

Two factors limit the minimum operating temperature of large area CCD detectors for visible wavelength. Detectors of this type frequently use doped polysilicon structure for the gate electrodes which control the manipulation of electrical charge within the array. At low temperature, carrier freeze-out causes a rapid increase in the resistance of the polysilicon structure and impairs operation of the device. An additional effect arises from the use of implantations and diffusions to form barriers to control the direction of charge flow in the CCD. At freeze-out temperatures such barriers become ineffective and device performance is further degraded.

The problems associated with the operation of CCD detectors in the low temperature environment of an infrared telescope were investigated in the laboratory.[7] Several conclusions were reached as a result of experiments using

**Table 4 Infrared telescope—FPS requirements**

| | |
|---|---|
| Number of guide-stars | $\leq 10$ |
| Field of view | 15 arcmin radius |
| Limiting star magnitude | 14 |
| Accuracy | $\pm 0.25$ arcsec |
| Stability | 0.25 arcsec ($1\sigma$) |
| Output data rate | 10-50/s |
| Max scan rate | 30 arcmin/s |
| Max space chop rate | 20 Hz |
| Chopping displacement | $\pm 7.5$ arcmin |
| Telescope aperture | 1.2 m ($f/7$) |
| Focal plane ambient temperature | 20 K |

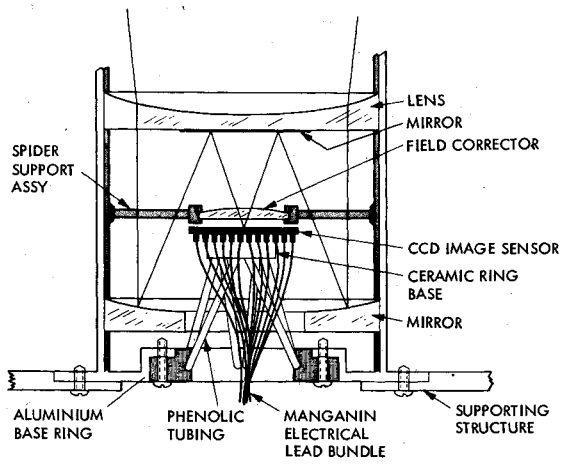


**Fig. 10 Single CCD configuration for infrared telescope application.**

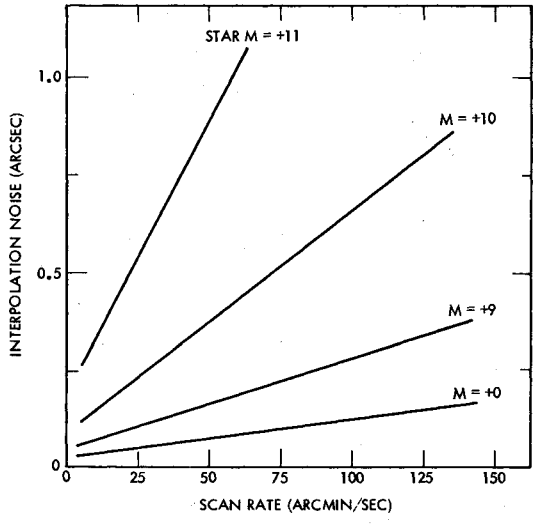


**Fig. 11 Calculated interpolation noise in the presence of scan-induced image smear.**

Fairchild CCD211 imaging arrays:

1) No evidence of mechanical weakness has been identified for temperatures as low as 20 K.

2) Excellent test pattern quality was obtained down to 77 K. Below this temperature, degradation of charge transfer efficiency in the horizontal register was observed with the devices becoming inoperable at 52 K.

3) Overall light response showed a change in light sensitivity and in the gain of the on-chip amplifier with maximum gain occurring at 70 K.

4) Dark current dropped steadily with temperature, becoming unmeasurable, in this experiment, below 200 K.

All measurements indicate this CCD will perform most satisfactorily in a focal plane sensor with detector temperatures as low as 80-100 K. An elevated CCD operating temperature (above 20 K) can be maintained without excessive heat input to the instrument area by means of a controlled conduction thermal isolation CCD mount (Fig. 10). The temperature differential between the detector and the telescope interface is established by the CCD dissipation and parasitic leadwire leakage without any need for additional electric heating. The elements and structure of the catadioptric tracker telescope provide containment and radiation shielding for the detector, thus preventing any detector-radiated energy from reaching the IR instruments.

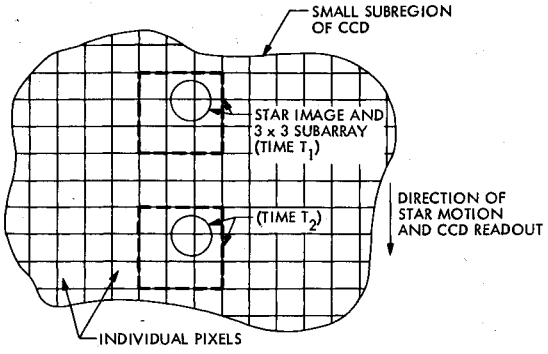


**Fig. 12 Smear reduction using synchronized CCD readout (3×3 pixel subarray is moved with star image).**

### Image Smear

Although the chop-mode can be readily accommodated by tracking both images of each guide-star, the measurement of pointing errors is considerably complicated by the presence of substantial image smear (scan mode). At least three tracking approaches are possible with selection depending to some extent on operational constraints. First, "normal" integration periods of 20 ms or more can be used. Since these intervals are long compared to the image motion rate, star images will be smeared by 10 or more pixels, requiring modified interpolation techniques. Figure 11 presents results of a noise analysis of this case, where a relatively simple centroid of brightness algorithm is used.

A second approach, using much shorter integration intervals (~2 ms) to confine smearing to one of two pixels, can be realized with some presently available CCD's. However, in general, it is not possible to increase the sample rate proportionally due to limitations in the readout speed of the CCD and the time required for error signal calculation.

A third, potentially powerful, means of dealing with image smear is available if the image motion can be confined to a predetermined direction parallel to the CCD columns. This technique involves synchronizing the CCD readout with the motion of the guide-star images (Fig. 12). As star images sweep across the image plane, the resulting charge image is stepped through the CCD at the same rate. Since the relative velocity between the optical and charge images is small, performance approaching the stationary tracking case can be achieved.

Tracking stability analyses were performed for the infrared telescope to model both staring and scanning pointing modes. These analyses indicate that the required accuracy and noise performance applicable to stationary pointing can be achieved with reasonable integration times. For example, under worst-case guide-star availability near the galactic pole, where there is an 85% probability of a star brighter than $m_v = 12$ in the tracking field, the sensor noise is 0.13 arcsec. The noise generally exceeds this limit in high-rate celestial scans greater than 50 arcmin/s when guiding on stars fainter than $m_v \sim 9$.

## Conclusion

Both fine pointing sensor examples described here illustrate the advantages of using CCD's for star tracking application. High accuracy, low noise, and the absence of moving parts are three of the strongest attributes of this approach. Perhaps the greatest weakness is that large-area CCD's are state-of-the-art devices with low production yields. As this situation improves, it can be expected that the role of CCD's in all star tracking applications will increase dramatically, including the fine pointing control of large telescopes.

## Acknowledgments

This paper presents the results of one phase of research conducted at the Jet Propulsion Laboratory, California

Institute of Technology, under NASA contract NAS7-100. The infrared telescope analysis and low temperature experiments were supported by the Ames Research Center as part of the Shuttle Infrared Telescope Facility (SIRTF) program. The authors are indebted to J. McLauchlan for the initial development of the multi-CCD FPS concept and for his support and direction during much of this work.

## References

[1] Lorell, K.R., Murphy, J.P., and Swift, C.D., "A Computer-Aided Telescope Pointing System Utilizing a Video Star Tracker," VII IFAC Symposium on Automatic Control in Space, Rottach-Egern FRG, May 1976.

[2] Goss, W.C., "CCD Star Trackers," Symposium on Charge-Coupled Device Technology for Scientific Imaging Applications, Pasadena, Calif., June 1975.

[3] Salomon, P.M. and Goss, W.C., "A Microprocessor-Controlled CCD Star Tracker," AIAA Paper 76-116, AIAA 14th Aerospace Sciences Meeting, Washington, D.C., Jan. 1976.

[4] Lorell, K.R., Barrows, W.F., and Lee, G.K., "Development of a Multistar Processing Algorithm for Use with a Focal Plane Fine Guidance Sensor," NASA TMX-78-563, April 1979.

[5] Wolfe, W.L. (ed.), *Handbook of Military Infrared Technology*, U.S. Office of Naval Research, Washington, D.C., 1965, p. 110.

[6] "UBV Sequences in Selected Areas," Vol. XX, Part VII, U.S. Naval Observatory, 1974.

[7] Hill, R.E., "Preliminary Design with Supporting Studies of a Focal Plane Guidance Sensor Using a Charge-Coupled Image Detector for the Space Shuttle Infrared Telescope Facility," JPL Doc. 760-177, May 1977.